Appendix for "When and How to Lift the Lockdown? Global COVID-19 Scenario Analysis and Policy Assessment using Compartmental Gaussian Processes"

Zhaozhi Qian[*]
University of Cambridge
zhaozhi.qian@maths.cam.ac.uk

Ahmed M. Alaa[*]
UCLA
ahmedmalaa@ucla.edu

Mihaela van der Schaar
University of Cambridge, UCLA, The Alan Turing Institute
mv472@cam.ac.uk

Appendix A: Related Literature

In this Section, we provide a detailed comparison between different existing approaches for modeling fatality curves. A tabulated comparison between our model and existing ones is laid out in Table A1.

Approach	**Training Approach**	**Modeling Scope**	**Policy Effects**	**Model Uncertainty**
Compartmental models	Exhaustive parameter search	Individual countries	Not incorporated	None
Machine learning-based compartmental models	Gradient descent optimization	Individual countries	Not incorporated	Ad-hoc bootstrap estimates
Bayesian mechanistic hierarchical model	Posterior inference via MCMC methods	Individual countries	Incorporated	Bayesian credible intervals
Curve fitting	Exhaustive parameter search	Individual countries	Not incorporated	None
Dynamic control modeling	Model parameters based on expert knowledge	Individual countries	Incorporated	None
Recurrent neural networks for fatality curve modeling [49]	Gradient descent optimization	Individual countries	Not incorporated	None
Compartmental Gaussian processes	**Stochastic gradient-based variational inference**	**Global**	**Incorporated**	**Bayesian credible intervals**

Table A1: Comparison between existing approaches to model fatality curves.

Because of the relative infrequency of pandemics, little related work has been done within the machine learning community to address this problem. In what follows, we provide a brief overview of previous works. Previous works prior to the current pandemic have been primarily focused on learning contagion (diffusion) processes on networks, e.g., [15, 16]; unfortunately, these models do

[*]Equal contribution.

34th Conference on Neural Information Processing Systems (NeurIPS 2020), Vancouver, Canada.

not apply to the pandemic as information on social network structures underlying disease spread is hard to obtain. In response to the COVID-19 pandemic, two strands of research work have emerged: (a) methods for devising optimal control (lockdown) policies to contain disease spread [17, 18, 19], and (b) models for forecasting disease spread and expected fatalities [5, 6, 7, 9, 10, 20, 21]. Our paper belongs to category (b) in that the developed model is trained to forecast the future number of fatalities. But unlike existing models in category (b), our model predicts fatalities under different lockdown policy choices, hence it can be used for research in category (a) to derive optimal policies.

The most prominent models in category (b) — developed by various academic institutions — have been recognized by the CDC and used to issue national forecasts of COVID-19 fatalities within the United States [22]. Most of these models (e.g., the "UCLA" model [9], the "MIT" model [21] and the IHME model [5]) are SEIR models fit for *individual* countries, with ideas from "machine learning" being used only to optimize the basic SEIR parameters via gradient descent. Our model differs from these models in that it: (1) jointly models fatalities across all of the 170 countries affected by the pandemic, (2) incorporates individual country features to learn how disease dynamics and policy effects vary across countries, (3) enables evaluating future projections under alternative policy scenarios, and (4) combines both mechanistic SEIR models and data-driven machine learning models. Hierarchical modeling has been previously used in the "Imperial" model developed in [20] (which was fit across 11 European countries). This model can be viewed as a special case of ours as it assumes policy effects to be fixed for all countries in its upper layer with no machine learning components to model heterogeneity, and its lower layer uses an interval distribution to predict short-term deaths only.

Appendix B: Learning via Stochastic Variational Inference

Accurate posterior inferences of $\mathcal{Y}_i[t:t+T]$ require training the CGP model by optimizing the parameter α of the upper-layer GP using the observed data $\mathcal{D}_{N,t}$ by maximizing the model's log-likelihood:

$$\mathcal{L}(\mathcal{D}_{N,t} \,|\, \alpha) \triangleq \log \int \prod_{i=1}^{N} \mathbb{P}\big(\, \mathcal{Y}_i[1:t] \,\big|\, \theta_i\big) \cdot \mathbb{P}\big(\, \theta_i \,\big|\, \boldsymbol{X}_i, \mathcal{P}_i[1:t], \alpha\big)\, d\theta_i, \tag{1}$$

with $\alpha^* = \arg\max_\alpha \mathcal{L}(\mathcal{D}_{N,t} \,|\, \alpha)$. Because the integral in (1) is intractable, we resort to a variational inference approach for optimizing the model's likelihood [32, 33, 34, 35]. That is, to train our model, we minimize the Evidence lower bound (ELBO) on (1) given by:

$$\log \mathbb{P}\big(\, \mathcal{Y}_i[1:t] \,\big|\, \alpha\big) \geq \text{ELBO}_i(\alpha, \phi) = \mathbb{E}_{\mathbb{Q}}\left[\log \mathbb{P}\big(\, \mathcal{Y}_i[1:t], \theta_i \,\big|\, \alpha\big) - \log \mathbb{Q}\big(\, \theta_i \,\big|\, \mathcal{Y}_i[1:t], \phi\big)\right],$$

where $\mathbb{Q}(.)$ is the variational distribution with parameters ϕ, and conditioning on $\boldsymbol{X}_i$ and $\mathcal{P}_i[1:t]$ is suppressed for notational brevity. We choose a normal distribution for $\mathbb{Q}(.)$ — this renders analytic evaluation of the ELBO objective and its gradients possible. We use stochastic gradient descent via ADAM algorithm to optimize the ELBO objective [36], and update the lower-layer parameters in each gradient iteration by solving the SEIR differential equations using Euler's method [37].

The pseudo-code for the learning algorithm is provided below:

1. Sample $\theta_i^{(j)} \sim \mathbb{Q}\big(\, \theta_i \,\big|\, \mathcal{Y}_i[1:t], \phi\big),\ i = 1, \ldots, N,\ j = 1, \ldots, m.$
2. Estimate $\mathcal{L}(\mathcal{D}_{N,t} \,|\, \alpha) = \log \sum_{j=1}^{m} \prod_{i=1}^{N} \mathbb{P}\big(\, \mathcal{Y}_i[1:t] \,\big|\, \theta_i^{(j)}\big) \cdot \mathbb{P}\big(\, \theta_i^{(j)} \,\big|\, \boldsymbol{X}_i, \mathcal{P}_i[1:t], \alpha\big)\, d\theta_i^{(j)}.$
3. Estimate the gradients $\nabla_\theta \mathcal{L}$ and $\nabla_\phi \mathcal{L}$.
4. Solve the SEIR differential equations using Euler's method.
5. Update θ and ϕ.

Appendix C: Experiments

Model Variables

We collated the data set $\mathcal{D}_{N,t} = \{\boldsymbol{X}_i, \mathcal{Y}_i, \mathcal{P}_i\}_{i=1}^{N}$ for $N = 170$ countries affected by the COVID-19 pandemic using three data sources: (1) published World Bank reports were used to extract a set of $d = 35$ features $\boldsymbol{X}_i$ for each country, (2) the COVID-19 CSSE data repository at Johns Hopkins University [38] was used to extract each country's fatality time-series $\mathcal{Y}_i$, and (3) the Oxford COVID-19 Government Response Tracker (OxCGRT) — curated by the Blavatnik School of Government at

Oxford University [39] — was used to extract $K = 9$ policy indicators $\mathcal{P}_i$ for each country over time. Our data set covered the period spanning from January 22, 2020 to May 8, 2020.

Each country's features included a comprehensive set of economic, demographic, environmental, social and health indicators (e.g., population density, prevalence of obesity, air transport frequency, median age, prevalence of hand-washing facilities, health expenditure, etc). Policy indicators included: information on school and workplace closure, public events' cancellation, travel restrictions, public transport closure, etc. All variables inlcuded in our model are listed in Tables C1 and C2.

I^0: School closure	I^1: Stay-at-home requirements	I^2: Restrictions on gathering size
I^3: Workplace closure	I^4: Restrictions on domestic or internal movement	I^5: Public transport closures
I^6: Cancellation of public events	I^7: Restrictions on international travel	I^8: Public information campaign

Table C1: Individual policy indicators used in our model.

Economic Indicators GDP per capita, GNI per capita, Income share held by lowest 20%
Social and Demographic Indicators Population, Life expectancy, Birth rate, Death rate, Infant mortality rate, Land Area, % People with basic hand-washing facilities including soap and water, Smoking prevalence, Prevalence of undernourishment, Prevalence of overweight, Urban population, Population density, Population ages 65 and above, Access to electricity (% of population), UHC service coverage index, Total alcohol consumption per capita, Air transport (passengers carried)
Environmental Indicators Forest Area, PM2.5 air pollution (mean annual exposure in micrograms per cubic meter)
Public Health Indicators Immunization for measles, % deaths by communicable diseases, Current health expenditure, Current health expenditure per capita, Diabetes prevalence, Immunization for DPT, Immunization for HepB3, Incidence of HIV, Incidence of malaria, Incidence of tuberculosis, % deaths by CVD/cancer/diabetes/CRD , % deaths due to household and ambient air pollution, % deaths due to unsafe water/unsafe sanitation/lack of hygiene, Physicians (per 1,000 people)

Table C2: Economic, social, demographic, environmental and health indicators for each country considered in our analysis. Data on these indicators was obtained from the World Bank (https://data.worldbank.org/).

Model Implementation Details

We implemented our CGP model using `Pyro` [40], a universal probabilistic programming language in Python supported by a PyTorch backend. The variational inference algorithm was implemented using ADAM with 1000 iterations and a learning rate of 0.01. The Gaussian process hyper-parameters were tuned by keeping the last 14 days worth of fatality data as a validation set, and grid search was used to tune the kernel hyper-parameters (length-scale). Projections from all baselines involved in our comparisons were obtained from the official CDC website [22].

Results

In this Section, we provide further experimental results in addition to those presented in Section 4. In what follows, we list the results provided in this appendix.

- **Table C3**: Performance of our model with and without cross-country joint modeling.
- **Table C4**: Correlation between country features and effect of lockdown on R_0.
- **Table C5**: Correlation between country features and R_0 before lockdown.
- **Table C8**: The difference in total deaths by April 25 as reported at April 25 and May 8.
- **Figure C6**: Policy stringency index (defined by te Oxford policy tracker [3]) and R_0 over time within different countries.
- **Figure C7**: Counterfactual scenario analysis for France. The blue curve corresponds to the current lockdown measures continuing, whereas the red curve corresponds to the current re-opening plan.

Country	4/25 - 5/01 (One week)					4/25 - 5/07 (Two weeks)				
	IHME	**YYG**	**Imperial**	**CGP (local)**	**CGP (global)**	**IHME**	**YYG**	**Imperial**	**CGP (local)**	**CGP (global)**
Austria	-26	15	1		-37	-	55	20		-39
Brazil	-	-283	-	454	-105	-	-768	-	3011	-298
Denmark	37	10	14		-5	-	2	4		-10
Egypt	-	-	-	-6	-47	-	-	-	25	-93
France	-501	803	-2415	1421	-79	-1412	1601	-1974	5246	-485
Germany	-420	244	-417	310	104	-661	628	-288	919	179
Iran	-	40	-	2	9	-	79	-	-93	9
Italy	-1082	451	1804	608	294	-2591	732	1600	1999	901
Japan	-	-	-	38	-3	-	-	-	92	-74
Mexico	-	-82	-	-99	-56	-	-518	-	-435	-315
Netherlands	512	172	265	256	-21	-	363	228	850	-47
Norway	29	20	-12	12	2	-	38	-7	45	12
Philippines	-	-21	-		-14	-	-70	-		-30
Poland	20	-8	-		14	-	3	-		2
Portugal	-28	41	28		4	-95	107	24		-3
Romania	-96	-1	-		-32	-236	-2	-		-64
South Africa	-	-	-	-4	-8	-	-	-	-36	-34
South Korea	-	-	-	7	3	-	-	-	24	11
Spain	1104	167	-499	568	317	102	76	712	575	50
Sweden	311	107	-102	-24	24	693	256	-35	-301	-7
Switzerland	30	14	-306		-87	-	97	-275		-154
Turkey	-	177	-		118	-	394	-		488
United Kingdom	-981	-3479	-182	226	-131	658	-3433	-29	1755	761
Russia	-	-119	-	-31	-155	-	-199	-	229	-307
India	-	-169	-	-18	-75	-	-630	-	-241	-420

Table C3: Performance of our model with and without cross-country joint modeling.

Country features	Correlations	p-values
Cause of death, by communicable diseases and maternal, prenatal and nutrition conditions (% of total)	0.732615	1.25E-06
Mortality rate attributed to unsafe water, unsafe sanitation and lack of hygiene (per 100,000 population)	0.667864	2.17E-05
Incidence of tuberculosis (per 100,000 people)	0.665138	2.41E-05
Prevalence of undernourishment (% of population)	0.659093	3.03E-05
Mortality rate, adult, female (per 1,000 female adults)	0.648255	8.03E-05
Mortality rate attributed to household and ambient air pollution, age-standardized (per 100,000 population)	0.642676	5.51E-05
Mortality rate, under-5 (per 1,000 live births)	0.60216	0.000209
Mortality rate, adult, male (per 1,000 male adults)	0.570695	0.000801
Mortality rate attributed to unintentional poisoning (per 100,000 population)	0.49254	0.003593
Mortality from CVD, cancer, diabetes or CRD between exact ages 30 and 70 (%)	0.459674	0.007117
Population, total	0.401973	0.0204
Birth rate, crude (per 1,000 people)	0.389252	0.025156
Mortality caused by road traffic injury (per 100,000 people)	0.36984	0.03414
PM2.5 air pollution, mean annual exposure (micrograms per cubic meter)	0.347458	0.047564
Urban population (% of total population)	-0.35538	0.042399
Current health expenditure per capita (current US$)	-0.37345	0.032298
Nurses and midwives (per 1,000 people)	-0.40256	0.020202
Current health expenditure (% of GDP)	-0.40361	0.019846
GNI per capita, Atlas method (current US$)	-0.40771	0.018513
GDP per capita (current US$)	-0.41523	0.016262
Immunization, HepB3 (% of one-year-old children)	-0.42523	0.024084
Physicians (per 1,000 people)	-0.48562	0.005616
Immunization, DPT (% of children ages 12-23 months)	-0.49294	0.003562
Immunization, measles (% of children ages 12-23 months)	-0.51081	0.002385
Life expectancy at birth, total (years)	-0.57085	0.000522
UHC service coverage index	-0.58407	0.000359
Prevalence of overweight (% of adults)	-0.61696	0.000131
Access to electricity (% of population)	-0.62433	0.000103
Cause of death, by non-communicable diseases (% of total)	-0.68116	1.28E-05
People with basic handwashing facilities including soap and water (% of population)	-0.8102	0.014751

Table C4: Correlation between country features and effect of lockdown on R_0.

Country feature	**Correlation**	p**-value**
People with basic handwashing facilities including soap and water (% of population)	0.73285	0.038626
Prevalence of overweight (% of adults)	0.576361	0.000447
UHC service coverage index	0.56557	0.000604
Cause of death, by non-communicable diseases (% of total)	0.546701	0.000995
Access to electricity (% of population)	0.503035	0.002847
Life expectancy at birth, total (years)	0.49019	0.003781
Physicians (per 1,000 people)	0.481126	0.006143
Current health expenditure (% of GDP)	0.448501	0.00885
Urban population (% of total population)	0.429586	0.012597
Immunization, measles (% of children ages 12-23 months)	0.419842	0.014999

Table C5: Correlation between country features and R_0 before lockdown.

Country	**Percentage Difference**	**Difference**
US	0.88%	456
France	0.14%	31
United Kingdom	0.00%	0
Pakistan	0.00%	0
Japan	0.00%	0
Italy	0.00%	0
Germany	0.00%	0
Spain	0.00%	0
Belgium	0.00%	0
Korea, South	0.00%	0
Brazil	0.00%	0
Iran	0.00%	0
Netherlands	0.00%	0
Turkey	0.00%	0
Romania	0.00%	0
Portugal	0.00%	0
Sweden	0.00%	0
Switzerland	0.00%	0
Ireland	0.00%	0
Hungary	0.00%	0
Denmark	0.00%	0
Austria	0.00%	0
India	0.00%	0
Ecuador	0.00%	0
Russia	0.00%	0
Peru	0.00%	0
Indonesia	0.00%	0
Poland	0.00%	0
Philippines	0.00%	0
Canada	-0.76%	-18

Table C8: The difference in total deaths by April 25 reported at April 25 and May 8. The difference is exactly zero for most countries; for countries with a difference, the difference is negligible percentage-wise. The models in our experiments were trained based on data captured at May 8 while the benchmarks were probably trained using data capture at April 25. As the data are routinely updated, we are expecting to see some occasional retrospective changes (e.g. correcting reporting errors). However, the vast majority of countries are *unchanged* between the two reporting dates, which suggests that our training scheme is valid.

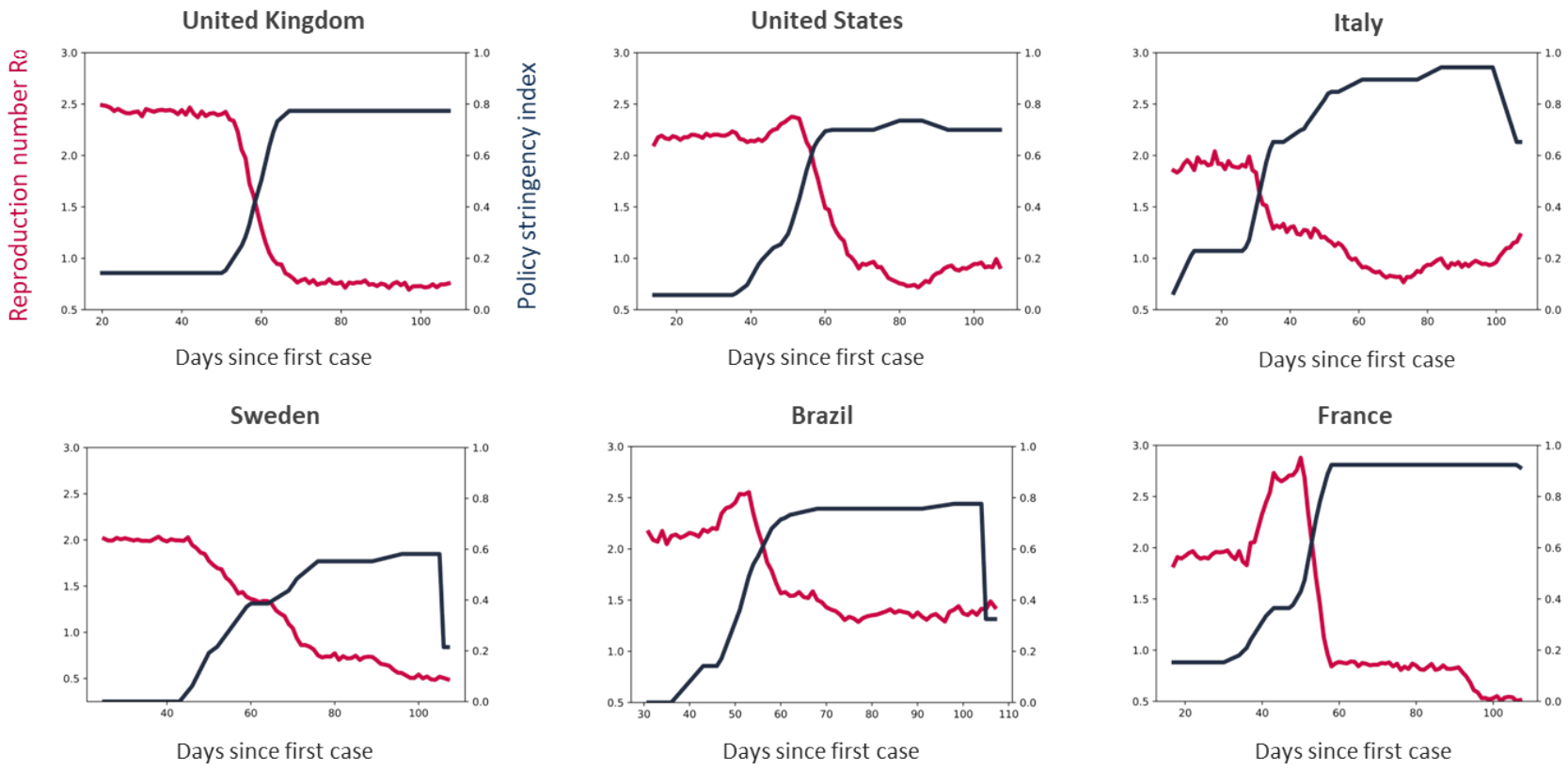

Figure C6: Policy stringency and R_0 over time within different countries.

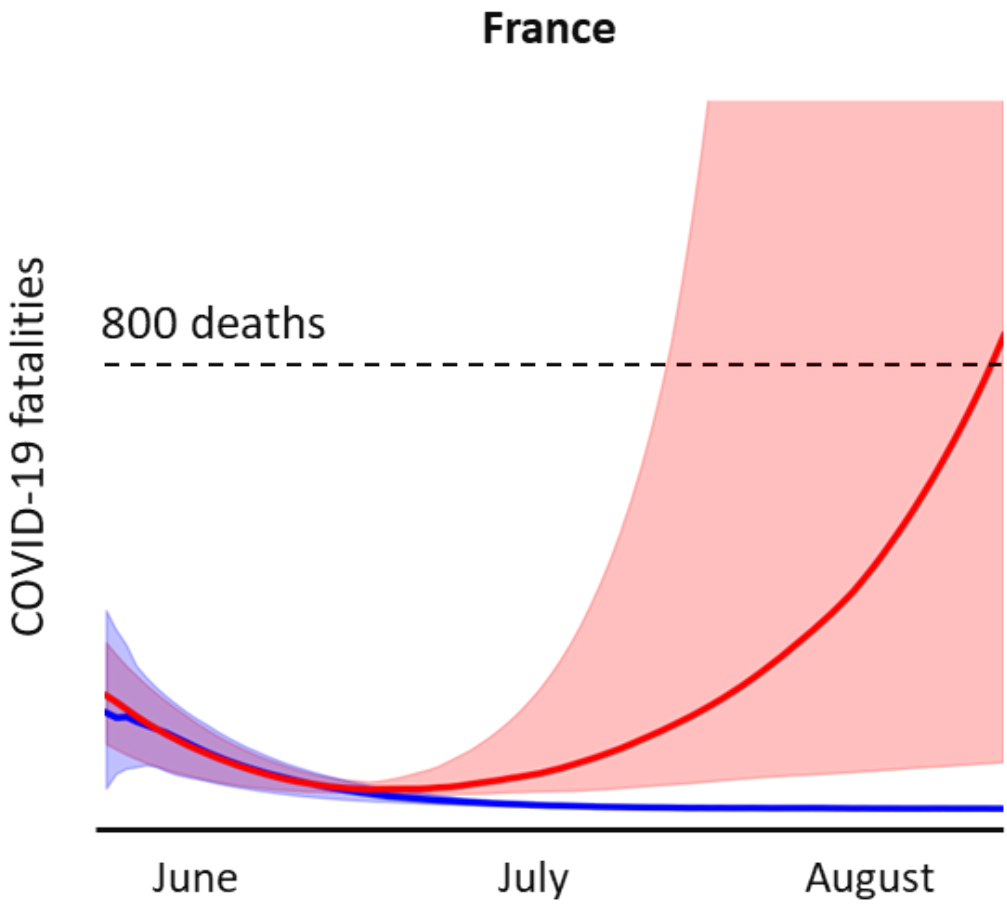

Figure C7: Counterfactual scenario analysis for France.

References

[1] K. Prem, et al. "The effect of control strategies to reduce social mixing on outcomes of the COVID-19 epidemic in Wuhan, China: a modelling study." *The Lancet Public Health*, 2020.

[2] N. M. Ferguson, D. Laydon, G. Nedjati-Gilani, et al. "Impact of non-pharmaceutical interventions (NPIs) to reduce COVID-19 mortality and healthcare demand." *Imp Coll COVID-19 Response Team*, 2020.

[3] T. Hale, A. Petherick, T. Phillips, and S. Webster. "Variation in government responses to COVID-19." *Blavatnik School of Government Working Paper*, 2020.

[4] F. E. Alvarez, D. Argente, and F. Lippi. "A simple planning problem for covid-19 lockdown." *National Bureau of Economic Research*, 2020.

[5] IHME COVID-19 health service utilization forecasting team and Christopher J. Murray. "Forecasting the impact of the first wave of the COVID-19 pandemic on hospital demand and deaths for the USA and European Economic Area countries." *medRxiv*, 2020.

[6] J. Lourenço, et al. "Fundamental principles of epidemic spread highlight the immediate need for large-scale serological surveys to assess the stage of the SARS-CoV-2 epidemic." *medRxiv*, 2020.

[7] P. Teles. "A time-dependent SEIR model to analyse the evolution of the SARS-covid-2 epidemic outbreak in Portugal." *Bull World Health Organ*, 2020.

[8] D. S. W. Ting, L. Carin, V. Dzau, and T. Y. Wong. "Digital technology and COVID-19." *Nature Medicine*, no. 26, vol. 4, pp. 459-461, 2020.

[9] D. Zou, L. Wang, P. Xu, J. Chen, W. Zhang and Q. Gu. "Epidemic Model Guided Machine Learning for COVID-19 Forecasts in the United States." *medRxiv*, 2020.

[10] Y. Gu. "COVID-19 Projections Using Machine Learning." covid19-projections.com, 2020.

[11] A. L. Andersen, et al. "Pandemic, Shutdown and Consumer Spending: Lessons from Scandinavian Policy Responses to COVID-19." *arXiv preprint arXiv:2005.04630*, 2020.

[12] M. Gilbert, M. Dewatripont, E. Muraille, J. P. Platteau and M. Goldman. "Preparing for a responsible lockdown exit strategy." *Nature Medicine*, vol. 26, no. 5, pp. 643-644, 2020.

[13] M. Y. Li and J. S. Muldowney. "Global stability for the SEIR model in epidemiology." *Mathematical biosciences*, vol. 125, no .2, pp. 155-164, 1995.

[14] K. Dietz. "The estimation of the basic reproduction number for infectious diseases." *Statistical methods in medical research*, pp. 23-41, 1993.

[15] R. Lemonnier, et al. "Tight bounds for influence in diffusion networks and application to bond percolation and epidemiology." *Advances in Neural Info. Process. Systems* (NeurIPS), 2014.

[16] D. B. Neill, and A. W. Moore. "A fast multi-resolution method for detection of significant spatial disease clusters." *Advances in Neural Information Processing Systems* (NeurIPS), 2004.

[17] G. Zaman, Y. H. Kang and I. H. Jung. "Optimal treatment of an SIR epidemic model with time delay." *BioSystems*, vol. 98, no. 1, pp. 43-50, 2009.

[18] D. M. Dave, A. I. Friedson, K. Matsuzawa and J. J. Sabia. "When do shelter-in-place orders fight COVID-19 best? Policy heterogeneity across states and adoption time." *National Bureau of Economic Research*, 2020.

[19] D. Acemoglu, V. Chernozhukov, I. Werning and M. D. Whinston. "A Multi-Risk SIR Model with Optimally Targeted Lockdown." *National Bureau of Economic Research*, 2020.

[20] S. Flaxman, et al. "Estimating the number of infections and the impact of non-pharmaceutical interventions on COVID-19 in 11 European countries.", *arXiv preprint*, 2020.

[21] COVIDAnalytics Team, "Overview of DELPHI Model V2.0." covidanalytics.io/DELPHI_documentation_pdf, 2020.

[22] www.cdc.gov/coronavirus/2019-ncov/covid-data/forecasting-us.html, last accessed: June 1, 2020.

[23] R. Li, S. Pei, B. Chen, et al. "Substantial undocumented infection facilitates the rapid dissemination of novel coronavirus (SARS-CoV2)." *Science*, 2020.

[24] C. E. Rasmussen, "Gaussian processes in machine learning." *Springer*, 2003.

[25] J. Q. Shi, R. Murray-Smith, and D. M. Titterington. "Hierarchical Gaussian process mixtures for regression." *Statistics and computing*, 2005.

[26] W. O. Kermack, and A. G. McKendrick. "A contribution to the mathematical theory of epidemics." *Proceedings of the Royal Society of London*, pp. 700-721, 1927.

[27] J. T. Wu, et al. "Nowcasting and forecasting the potential domestic and international spread of the 2019-nCoV outbreak originating in Wuhan, China: a modelling study." *The Lancet*, 2020.

[28] H. W. Hethcote, "The mathematics of infectious diseases." *SIAM review*, pp. 599-653, 2000.

[29] A. Osemwinyen and A.Diakhaby. "Mathematical Modelling of the Transmission Dynamics of Ebola Virus." *Applied and Computational Mathematics*, 2015.

[30] S. A. Lauer, et al. "The incubation period of coronavirus disease 2019 (COVID-19) from publicly reported confirmed cases: estimation and application." *Annals of internal medicine*, vol. 172, no. 9, pp. 577-582, 2020.

[31] A. J. Kucharski, T. W. Russell, C. Diamond, et al. "Early dynamics of transmission and control of COVID-19: a mathematical modeling study." *Lancet Infect Dis*, 2020.

[32] M. D. Hoffman, D. M. Blei, C. Wang and J. Paisley. "Stochastic variational inference." *The Journal of Machine Learning Research*, vol. 14, no. 1, pp. 1303-1347, 2013.

[33] D. Wingate and T. Weber. "Automated variational inference in probabilistic programming." *arXiv preprint arXiv:1301.1299*, 2013.

[34] R. Ranganath, S. Gerrish, and D. M. Blei. "Black Box Variational Inference." *In Proceedings of the International Conference on Artificial Intelligence and Statistics (AISTATS)*, 2014.

[35] D. P. Kingma and M. Welling. "Auto-encoding Variational Bayes." *arXiv preprint*, 2013.

[36] D. P. Kingma and J. Ba. "Adam: A method for stochastic optimization." *arXiv preprint*, 2014.

[37] M. Hutzenthaler, A. Jentzen, and P. E. Kloeden. "Strong and weak divergence in finite time of Euler's method for stochastic differential equations with non-globally Lipschitz continuous coefficients." *Proceedings of the Royal Society A: Mathematical, Physical and Engineering Sciences*, vol. 467, no. 2130, pp. 1563-1576, 2011.

[38] JHU CSSE. 2019 Novel Coronavirus COVID-19 (2019-nCoV) Data Repository by Johns Hopkins CSSE. GitHub. 2020 (https://github.com/CSSEGISandData/COVID-19).

[39] T. Hale, A. Petherick, T. Phillips, and S. Webster. "Variation in government responses to COVID-19." *Blavatnik School of Government Working Paper*, 2020.

[40] E. Bingham, et al. "Pyro: Deep universal probabilistic programming." *The Journal of Machine Learning Research*, vol. 20, no .1, pp. 973-978, 2019.

[41] C. P. Winsor. "The Gompertz curve as a growth curve." *Proceedings of the National Academy of Sciences of the United States of America*, vol. 18, no. 1, 1932.

[42] www.economist.com/early-projections-of-covid-19-in-america-underestimated-its-severity

[43] https://covid-19.bsvgateway.org/, last accessed: June 1, 2020.

[44] A Azad. "Model cited by white house says 82,000 people could die from coronavirus by august, even with social distancing.", *CNN*, 2020. https://www.cnn.com/2020/03/30/health/coronavirus-us-ihme-model-us/index.html, last accessed: June 1, 2020.

[45] https://www.bbc.co.uk/news/health-52849691, last accessed: June 1, 2020.

[46] https://www.bbc.co.uk/news/uk-52858392, last accessed: June 1, 2020.

[47] https://www.telegraph.co.uk/global-health/science-and-disease/road-lockdown-sage-minutes-reveal-best-worst-whitehall/ , last accessed: June 1, 2020.

[48] https://www.gov.uk/government/publications/our-plan-to-rebuild-the-uk-governments-covid-19-recovery-strategy/, last accessed: June 2, 2020.

[49] S. K. Bandyopadhyay and S. Dutta. "Machine learning approach for confirmation of covid-19 cases: Positive, negative, death and release." *medRxiv*, 2020.